The role of structural heterogeneity in the homodimerization of transmembrane proteins **⑤**⊘

Ayan Majumder 📵 ; John E. Straub 🔀 📵



J. Chem. Phys. 159, 134101 (2023) https://doi.org/10.1063/5.0159801





CrossMark

Articles You May Be Interested In

A functional integral formalism for quantum spin systems

J. Math. Phys. (July 2008)

Modes selection in polymer mixtures undergoing phase separation by photochemical reactions

Chaos (June 1999)

Spreading of a surfactant monolayer on a thin liquid film: Onset and evolution of digitated structures

Chaos (March 1999)

500 kHz or 8.5 GHz? And all the ranges in between.

Lock-in Amplifiers for your periodic signal measurement









The role of structural heterogeneity in the homodimerization of transmembrane proteins 🕕

Cite as: J. Chem. Phys. 159, 134101 (2023); doi: 10.1063/5.0159801 Submitted: 26 May 2023 · Accepted: 27 July 2023 ·









Published Online: 2 October 2023

Ayan Majumder (D) and John E. Straub (D)



AFFILIATIONS

Department of Chemistry, Boston University, 590 Commonwealth Avenue, Boston, Massachusetts 02215, USA

a) Author to whom correspondence should be addressed: straub@bu.edu

ABSTRACT

The equilibrium association of transmembrane proteins plays a fundamental role in membrane protein function and cellular signaling. While the study of the equilibrium binding of single pass transmembrane proteins has received significant attention in experiment and simulation, the accurate assessment of equilibrium association constants remains a challenge to experiment and simulation. In experiment, there remain wide variations in association constants derived from experimental studies of the most widely studied transmembrane proteins. In simulation, state-of-the art methods have failed to adequately sample the thermodynamically relevant structures of the dimer state ensembles using coarsegrained models. In addition, all-atom force fields often fail to accurately assess the relative free energies of the dimer and monomer states. Given the importance of this fundamental biophysical process, it is essential to address these shortcomings. In this work, we establish an effective computational protocol for the calculation of equilibrium association constants for transmembrane homodimer formation. A set of transmembrane protein homodimers, used in the parameterization of the MARTINI v3 force field, are simulated using metadynamics, based on three collective variables. The method is found to be accurate and computationally efficient, providing a standard to be used in the future simulation studies using coarse-grained or all-atom models.

Published under an exclusive license by AIP Publishing. https://doi.org/10.1063/5.0159801

INTRODUCTION

Membrane proteins represent an important class of biomolecules responsible for the regulation of the structure and function of the cell. Most membrane proteins contain one or more transmembrane (TM) domains that span the bilayer or a single membrane leaflet. The association of TM regions plays a key role in determining the structure of the full protein.² Membrane proteins also play an important role in amyloid protein formation and association leading to Parkinson's disease³ and Alzheimer's disease.4 In this context, it is important to study the dimeric states of TM proteins to elucidate the possible modes of interaction defining their structural ensembles. Protein association in the membrane has been extensively studied using molecular dynamics simulation. However, slow diffusion in the membrane and the need to explore multiple substates defining the dimer ensemble present significant challenges to existing enhanced sampling methods.8

Coarse-grained models are commonly used to study the TM protein association on timescales beyond those accessible to all-atom simulations. 9-12 Enhanced sampling methods such as metadynamics, 9,13 umbrella sampling, 12,14 and adaptive biasing force¹⁵ have been extensively used to calculate the potential of mean force (PMF) of protein-protein and protein-lipid interactions using all-atom¹⁶ and coarse-grained models. ^{10–12} In these enhanced sampling methods, a collective variable (CV) or reaction coordinate must be defined connecting the initial and final configurations, such as the dimer and monomer states. The probability density along with the CV is then used to calculate the PMF. The most commonly used CVs in the study of homodimerization of TM proteins are the center-of-mass distance between two TM helices $(D_{com})^{11,17}$ and the distance root-mean-square displacement (D_{rmsd}) . ^{10,16} We have previously shown that the use of the one-dimensional CVs D_{com} and D_{rmsd} fail to sample all thermodynamically relevant states using umbrella sampling, leading to an overestimation of the binding free energy.¹² To address these shortcomings, we performed simulations exploring two CVs: the *x*-projection and *y*-projection of the center-of-mass distance between the two TM helices. The resulting two-dimensional PMF captures multiple homodimer substates missed by sampling based on standard one-dimensional CVs, leading to more accurate estimates of equilibrium binding constants. While effective, this approach is more computationally expensive than its one-dimensional counterpart and can be challenging to implement.

In this study, we propose a new protocol for the characterization of transmembrane protein association using well-tempered metadynamics. We demonstrate that this method leads to an accurate characterization of the free energy landscape defining the homodimerization equilibrium. We compare the results of this method with those derived from unbiased molecular dynamics simulations. The set of local minima observed in the unbiased simulations match those derived from the 3D metadynamics calculations. This good agreement between the two approaches suggests that the 3D metadynamics approach results in effective sampling of the thermodynamically relevant dimer structures. Taken together, these results demonstrate that the proposed method is a powerful tool to study the large-scale simulation of protein–protein association in membranes.

METHODS

The homodimerization of three transmembrane (TM) proteins, Glycophorin A (GpA), EphA1, and WALP23, was studied. The structures of GpA and EphA1 were taken from 1AFO¹⁹ and 2K1L,²⁰ respectively. Residues 69 to 97 of GpA were placed in a membrane bilayer composed of 404 POPC lipid molecules. The temperature of the simulation was maintained at 310 K. Residues 544 to 572 of EphA1 were embedded in a bilayer consisting of 406 DLPC molecules, and the simulations were performed at 303 K. WALP23 was studied in two bilayers, one composed of monounsaturated POPC and another of diunsaturated DOPC. Both lipid bilayers consisted of 406 lipid molecules. The temperature of the simulation was maintained at 310 K using the velocity rescale thermostat. The N-terminus of each protein was placed in the upper leaflet. All bilayer compositions studied are listed in supplementary material Table 1. Each bilayer was solvated with 12 MARTINI v3 water beads per lipid molecule and a salt (NaCl) concentration of 150 mM. The MARTINI v3 force field was used to simulate the protein embedded membrane bilayer.²¹ The simulation parameters were used in accordance with the recommendations for the MARTINI v3 force

Well-tempered metadynamics was employed with three CVs: the x-projection and y-projection of the center-of-mass (COM) distance of the two helices and the torsional angle as collective variables (Fig. 1). A Gaussian of height 0.1 kJ/mol was added after every 2000 steps using a multiple walker setup. A Gaussian width of 0.2 nm along x-projection and y-projection of the COM distance between two helices and 0.03 radian along the torsional angle was used. A bias factor value of 10 was used in each metadynamics simulation. The angular motion of one of the helices was restrained using a harmonic potential with a force constant of 2000 kJ mol $^{-1}$ rad $^{-2}$. To restrain the helix, a residue (ResX) was chosen, and a harmonic potential was applied to the angle between the COM X -ResX vector

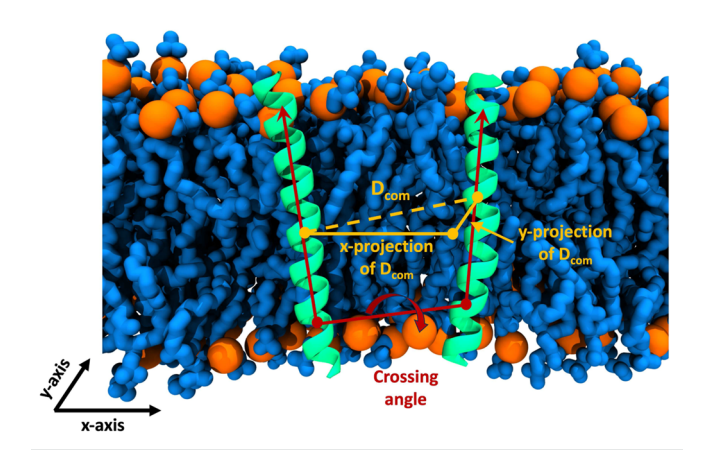


FIG. 1. Schematic representation of three CVs used in this work: the *x*-projection and *y*-projection of the center-of-mass (COM) distance of the two helices and the dihedral angle, referred to as the helical crossing angle.

and the positive x-axis. Here, the COM^X was defined as the center-of-mass of the residues from X-2 to X+2. Gly79, Gly554, and Ala11 were used as ResX to restrain the GpA, EphA1, and WALP23, respectively. Convergence of the three-dimensional PMFs obtained from the metadynamics simulations was accessed by projecting the PMF along the lateral COM–COM distances (D_{com}) between the two helices. In addition, a two-dimensional PMF was calculated using umbrella sampling (US) along the x-projection and y-projection of the COM–COM distances between the two helices. A detailed description of the method used to calculate the 2D PMF was provided in a previous study. All simulations were performed using the PLUMED v2.6.3²² and GROMACS 2018.3 programs.

RESULTS AND DISCUSSION

We used metadynamics simulations to quantify the dimerization kinetics of GpA, EphA1, and WALP23 homodimers in membrane bilayers. These protein homodimers have been extensively studied computationally and experimentally, and are wellestablished systems for benchmarking new methodologies. Metadynamics was used to calculate the PMF along the *x*-projection and y-projection of the COM-COM distance and the crossing angle between the helices. The projection of the computed 3D PMF onto the xy-plane (D_{xy}) is shown in Fig. 2. One of the helices that was centered on the xy-plane and the director vector, as defined in the "Methods section," was aligned with the positive x-axis. The PMF presents multiple minima, demonstrating that both GpA and EphA1 have multiple stable interaction sites. The free energy difference between the most stable homodimer structure and the dissociated state of the protein was found to be -8.5 and -5 kcal/mol for GpA and EphA1, respectively. WALP23 was studied in membranes consisting of pure POPC or DOPC lipids to understand the effect of lipid composition on protein association. The WALP23 dimer interaction was found to be specific, with similar intermolecular interactions observed in the presence of both lipids. The global minimum on the xy-plane for the WALP23 dimerization was found to be -5.5 and -4.4 kcal/mol in POPC and DOPC, respectively.

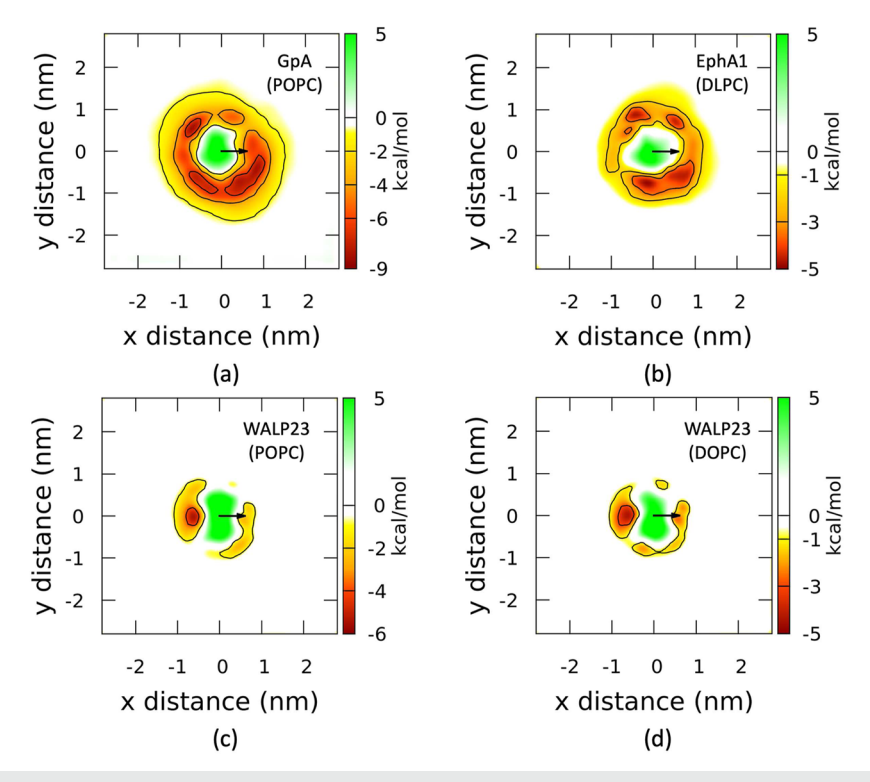


FIG. 2. Projection of the 3D PMF on the *xy*-distance between the COM of the TM helices for dimer formation of (a) GpA in POPC, (b) EphA1 in DLPC, WALP23 in (c) POPC, and (d) DOPC. The COM of one of the helices is centered in the *xy*-plane, and the black arrow represents the COM⁷⁹-to-Gly79 vector in GpA, the COM⁵⁵⁴-to-Gly554 vector in EphA1, and the COM¹¹-to-Ala11 vector for WALP23. The maximum value of the PMF was set to zero.

The free energy of dimerization of GpA, EphA1, and WALP23 has been measured by several experimental and computational studies. The reported values of the free energy of dimerization of GpA, measured using a variety of means, vary from 3.4 to 12.1 kcal/mol.²⁷⁻³² Computational studies employing a onedimensional CV have reported the free energy of dimerization of GpA to range from 3.0 to 11.5 kcal/mol. 16,17,33,34 In contrast, the 2D US calculation, using the MARTINI v2 force field, predicted the free energy of association to be 7.5 kcal/mol.¹² The dimerization free energy of EphA1, obtained from simulations using MARTINI v2, has been reported to be 7.7¹¹ and 7.8 kcal/mol.³⁵ In contrast, experimental FRET-based studies have reported the free energy of association to be 3.7 kcal/mol in DMPC.36 Castillo et al. found that the dissociation free energy of WALP23 is 4.8 kcal/mol in DOPC at 325 K.²⁵ Marrink and coworkers calculated the equilibrium association constant of WALP23 in di-C18:2 PC by quantifying the number of moles of dimers and monomers, resulting in a dimerization free energy value of 2.9 kcal/mol.³⁷ An experimental study of a similar system (AALALAA)₃ in di-C18:1 PC reported the free energy of dimerization to be 3 kcal/mol.³⁸ In the recent development of the MARTINI v3 force field by Souza et al., these four systems were used to validate the protein force field. The dimerization free energy of GpA in POPC, EphA1 in DLPC, and WALP23 in POPC and DOPC using the MARTINI v3 force field was found to be 5.9, 4.7, 2.9, and 2.6 kcal/mol, respectively.²¹

We calculated the binding constant and dimerization free energy of all systems studied. To calculate the binding constant, the 3D PMFs obtained from the metadynamics simulations were projected onto D_{com} (Fig. 3). The resulting PMFs along D_{com}

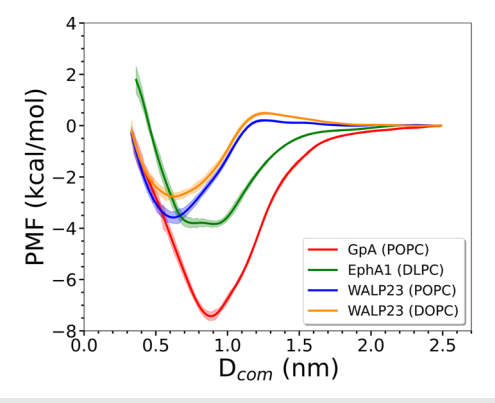


FIG. 3. Projection of the 3D PMF onto the one-dimensional CV D_{com} for the homodimerization of GpA in POPC, EphA1 in DLPC, WAPL23 in POPC, and DOPC. The maximum value of the PMF was set to zero. The error bar associated with each PMF was calculated using block analysis.

TABLE I. Minimum of the PMF (ΔW_{min}) along D_{xy} and D_{com}, and dimerization free energy (ΔG) obtained from the metadynamics simulations.

Protein	ΔW_{\min} (D _{xy}) (kcal/mol)	$\Delta W_{\min} (D_{com})$ (kcal/mol)	ΔG (kcal/mol)
GpA (POPC)	-8.5	-7.3 ± 0.1	-7.0 ± 0.1 -3.8 ± 0.1 -3.2 ± 0.2 -2.6 ± 0.1
EphA1 (DLPC)	-5.0	-3.8 ± 0.1	
WALP23 (POPC)	-5.5	-3.6 ± 0.2	
WALP23 (DOPC)	-4.4	-2.8 ± 0.1	

were then integrated over to obtain binding constant (K_D) , $^{34,39-41}$ where

$$K_D = \frac{1}{2} \times \frac{2\pi}{A_0} \int_0^{r_c} r e^{-\Delta W(r)/k_B T} dr.$$
 (1)

The standard reference area (A_0) was defined to be $1 \, \mathrm{nm}^2$. The cutoff distance (r_c) of 2.3 nm was chosen to define the associated and dissociated states of the protein homodimers. An entropic term $k_B T \ln(r)$ was included in $\Delta W(r)$ to account for the increasing accessible area with the increase in r. $^{16.42}$ The PMF reached a plateau above the cutoff distance, and this was set to zero. Values of the thermodynamic constants obtained from the simulation are presented in Table I. The dimerization free energy obtained for all the proteins studied using 3D metadynamics was found to be in line with the available experimental data.

To compare the results obtained from the 3D metadynamics simulations with the previously proposed 2D US method, we calculated a PMF over the xy-plane defined by the x-projection and y-projection of the COM-COM distances between the two helices. The 2D PMF obtained for the GpA homodimer using US is shown in supplementary material Fig. 1. The results demonstrate that 2D US captures the thermodynamically important substates of the GpA predicted by metadynamics. In addition, similar dimerization free energies were obtained from both 3D metadynamics and 2D US. We performed 2D US with dimers separated by 0.2 nm in each dimension. A total of ~700 independent 2 µs US window simulations were performed to reach convergence. In this study, we performed 4 µs simulations per umbrella to prepare a 2D PMF. A 3D PMF computed using metadynamics required ~180 μs of simulation (supplementary material Fig. 2) compared to a minimum of 1400 μ s of simulation needed for the 2D US. In order to perform a US, the protein dimer must be prepared according to the minimum of the external harmonic potentials. This process could be tedious compared to a metadynamics simulation that can be performed starting from any equilibrium conformation of the protein homodimer.

Many studies have been conducted to understand the structure of protein dimers in membrane. Structures obtained from molecular dynamics simulation can be compared with those derived from experiment to calibrate a model. Minima of the one-dimensional PMFs have been analyzed to evaluate the homodimer structures corresponding to the observed free energy minima. However, in many cases, the simulation along the 1D CV was found to be trapped in

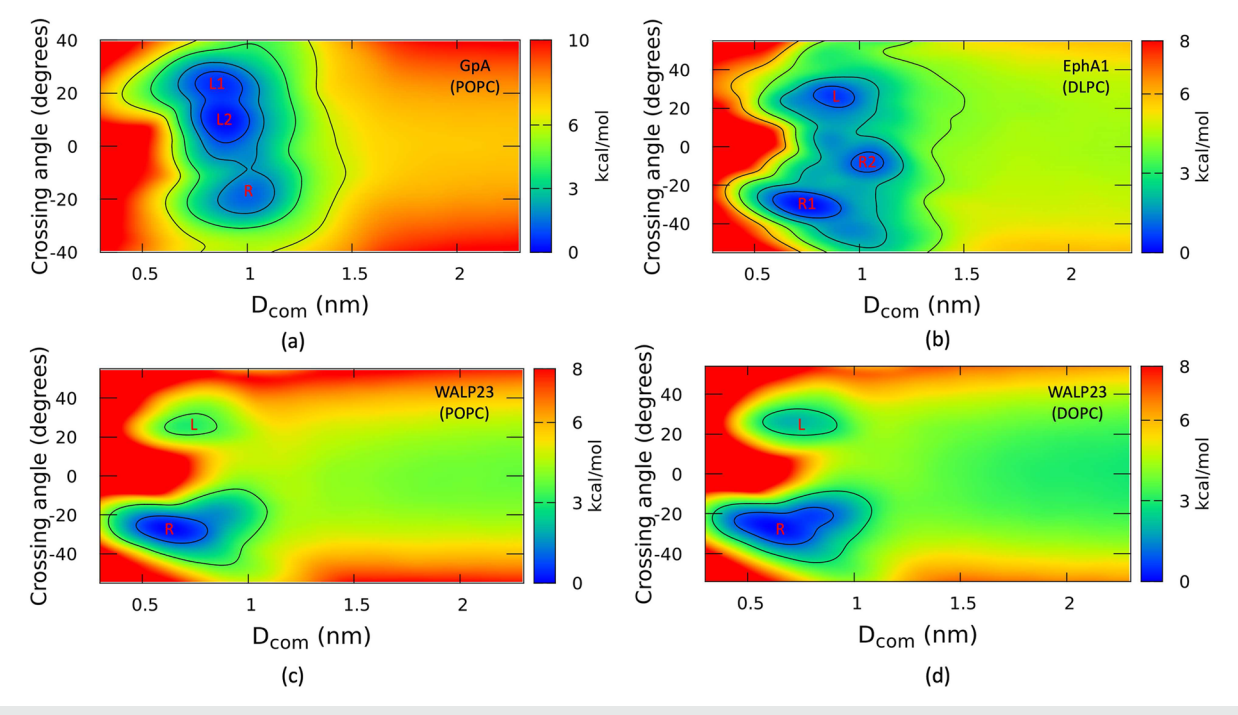


FIG. 4. Projection of the 3D PMF onto the crossing angle and D_{com} space for the dimer formation of (a) GpA in POPC, (b) EphA1 in DLPC, WAPL23 in (c) POPC, and (d) DOPC. The names of the different structural clusters (L or R) were assigned according to the distribution of crossing angle. The minimum value of the PMFs was set to zero.

local energy minima, restricting the sampling to only a subset of relevant conformations. We have previously shown that although 1D US samples only one minimum free energy structure, there exist other low free energy structures that are thermodynamically significant in computing the homodimerization equilibrium constant.

Experimental studies on GpA homodimer using x-ray crystal-lography⁴³ and nuclear magnetic resonance (NMR) spectroscopy¹⁹ have shown that key interactions stabilizing the dominant homodimer structures involve the glycine zipper motif (GXXXG). Those interactions stabilize a right-handed homodimer structure with a

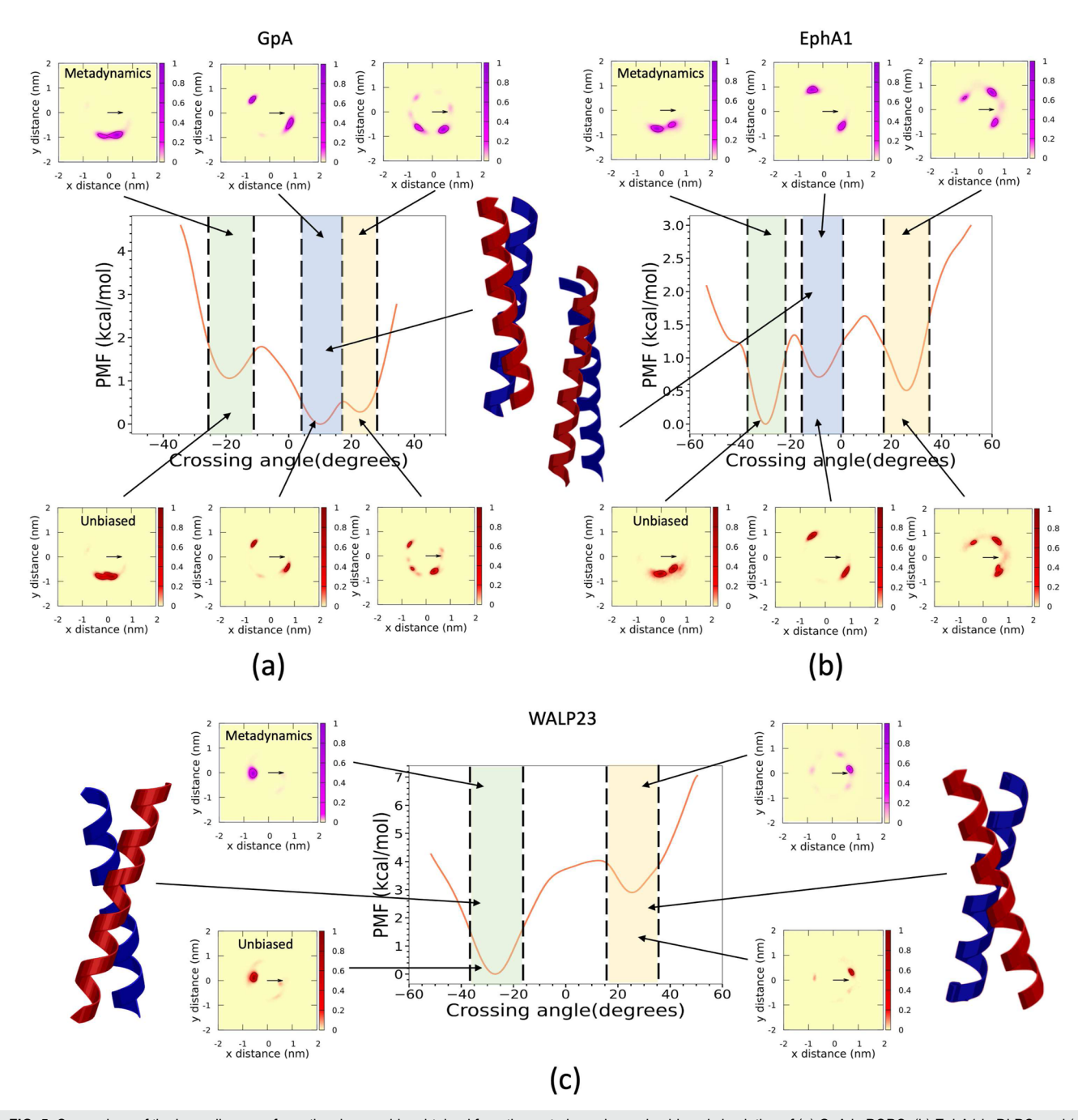


FIG. 5. Comparison of the homodimer conformational ensemble, obtained from the metadynamics and unbiased simulation of (a) GpA in POPC, (b) EphA1 in DLPC, and (c) WALP23 in POPC. The probability density along the *xy*-plane obtained from the metadynamics and unbiased simulation is shown in purple and red colorbars, respectively. PMF along the crossing angle was obtained from the metadynamics simulation.

crossing angle of -20° . A previous study using the MARTINI v2 model showed that the GpA interaction is mediated by the $G_{79}XXXG_{83}XXXT_{87}$ motif and forms a right-handed dimer with a -26° crossing angle. Similar studies using the MARTINI model have shown that the homodimer of EphA1 is stabilized by interactions facilitated by the glycine zipper motif, consistent with right-handed structures with a crossing angle of -20° .

To identify the interactions responsible for the crossing angles of thermodynamically stable homodimer structures, we projected the 3D PMF onto the crossing angle and D_{com} (Fig. 4). Minima on the free energy landscapes of the GpA and EphA1 homodimers were associated with three different average crossing angles. GpA was predicted to form a right-handed structure (cluster R) with a crossing angle of -22°, and two left-handed helical structures (clusters L1 and L2) with crossing angles of 22° and 5°, respectively. EphA1 was found to form two different right-handed structures (cluster R1 and R2) with crossing angles of -33° and -5° , respectively. In addition, a left-handed helix (cluster L) was observed to have a crossing angle of 30°. WALP23 preferentially forms right-handed structures (cluster R) in both POPC and DOPC with a crossing angle of -22°. However, a shallow basin in the PMF with a crossing angle of 22° suggests the presence of a relevant left-handed structure (cluster L). A recent study on GpA and EphA1 by Sahoo et al. employing the MARTINI v3 model identified three structural ensembles for each protein homodimer, where each ensemble is characterized by a different range of crossing angles. Our work is consistent with their observations.44

Unbiased simulations of GpA in POPC, EphA1 in DLPC, and WALP23 in POPC were performed for comparison with metadynamics simulations. Trajectories of the unbiased simulations were often observed to be trapped in local energy minima (supplementary material Fig. 3). To address this shortcoming, we performed 25 independent 5 μ s simulations. All simulations were initiated with the two TM protein helices, separated by a minimum of 2.5 nm, to study spontaneous homodimerization. While a PMF was not derived from the unbiased simulations, thermodynamically relevant structural conformations were identified. The probability distributions over the crossing angle and D_{com} obtained from the unbiased simulations are shown in supplementary material Fig. 4. The structural ensembles obtained from the unbiased simulations were found to be similar to those resulting from the 3D metadynamics simulations.

We identified key intermolecular interactions responsible for the observed handedness of the homodimers. The probability densities of these key intermolecular interactions are shown in Fig. 5. The complementary probability density was also calculated from the unbiased simulations. The conformational ensembles obtained from metadynamics and unbiased simulations were found to be comparable. In addition, we divided the ensemble into clusters of unique handedness and computed contact maps characterizing these key intermolecular interactions in each cluster. The contact maps of the homodimer structures of GpA, EphA1, and WALP23 are shown in supplementary material Figs. 5-7, respectively. In the case of GpA, three different homodimer conformations were found in the L1 cluster. Interaction between Ile76-Gly83-Thr87 of one helix and Thr74-Met81-Ile85 of the other helix form the L2 cluster. The glycine zipper motif interaction was observed in the right-handed helical structures (R cluster). While each unbiased simulation typically samples one conformation, we observed three distinct structures in the L1 cluster

in contrast to only one structure in other clusters (supplementary material Fig. 5). EphA1 also forms a right-handed helix, stabilized by interactions facilitated by the glycine zipper motif. Interaction between Val549-Phe553 and Gly554-Gly558 was observed in cluster R2. Two different structures were found in the L cluster. The Leu561-Gly564 of one helix interacts with the Leu562-Ile565 of the other helix and Gly558-Leu562 of one helix interacts with Leu557-Ala560 of other helix to form those left-handed structures observed in EphA1. WALP23 predominantly forms right-handed structures stabilized by interactions facilitated by the Ala9-Ala13-Ala17 motif. In contrast, the Ala7-Ala11 motif was found to interact to stabilize a left-handed structure.

Taken together, these results demonstrate that the proposed protocol involving metadynamics sampling over three collective variables, the *xy*-dimensions, and the helical tilt, exhaustively samples the thermodynamically relevant conformations contributing to the equilibrium homodimer association constant.

CONCLUSIONS

The past use of umbrella sampling over previously proposed one-dimensional collective variables has failed to adequately sample the homodimer ensemble for transmembrane homodimerization of GpA, EphA1, and WALP23. The resulting inadequate sampling has led to erroneous estimates of equilibrium association constants. To address this shortcoming, in this study we propose that a computational protocol based on metadynamics, employing three collective variables, defined as the *x*-projection and *y*-projection of the helical center-of-mass (COM) distance and the torsional angle between the helix vectors, is found to be more computationally efficient than umbrella sampling over the *xy*-dimensions.

Consider the case of homodimerization of GpA, perhaps the most intensely studied transmembrane protein homodimerization. There exists a wild variation in experimentally measured association constants, with associated free energies ranging from 3.4 to 12.1 kcal/mol. ^{27–32} Previous studies have suggested that non-native states do not make thermodynamically significant contributions to the association constant. ¹⁶ In contrast, our study suggests that native and non-native states in the homodimer ensemble must be included in an accurate calculation of equilibrium constants for transmembrane protein association.

While this study has focused on simulations using the MAR-TINI v3 force field, the computational protocol is readily applicable to all-atom simulations. Currently, there is evidence that top-down, coarse grained models may provide a more accurate assessment of transmembrane homodimer formation than all-atom models. Employing the computational protocol developed in this study, it should be possible to efficiently determine accurate association constants from all-atom simulations for critical comparison with experiment. Calculations of that kind could form the basis for enhancements in the parameterization of all-atom force fields for membrane protein simulation.

In this work, we include the contributions of the observed native and non-native states in the calculation of K_D . However, depending on the details of the experimental method employed, it is possible that the measured K_D would include only the native state or the native state and a subset of non-native states. Given a clear identification of the dimer states probed in an experiment and a

multidimensional PMF of the kind presented in this study, the integration involved in the calculation of K_D can be restricted in a way that provides a more precise correspondence between theory and experiment.

In addition, our work has primarily focused on the use of K_D values derived from FRET experiments. In those experiments, peptides are labeled with donor and acceptor moieties that may contribute to the PMF and the observed binding constant. A more exact comparison of theory and experiment would involve a determination of the PMFs for the modified proteins, including the donor and acceptor labels, and an appropriate weighting of the distance dependence. This is feasible and could be addressed in the future studies.

This study establishes an effective computational protocol for the accurate calculation of equilibrium association constants for a given coarse-grained potential function. There is a need for similarly reproducible and accurate experimental estimates of association constants for transmembrane protein association. That knowledge is essential for the accurate parameterization and validation of computational models, and the assessment of time scales and mechanisms for protein association involved in recognition and signaling.

SUPPLEMENTARY MATERIAL

The supplementary material contains system compositions simulated in this study, comparison of the 2D US and 3D metadynamics, convergence of 3D PMFs, post analysis of unbiased simulations, and contact maps of GpA, EphA1, and WALP23.

ACKNOWLEDGMENTS

The authors thank Paulo Telles De Souza and Matthias Buck for sharing unpublished results and valuable conversations, and Conor B. Abraham for carefully reading the manuscript. The authors gratefully acknowledge the generous support of the National Institutes of Health (Grant No. R01 GM107703), National Science Foundation (Grant No. CHE1900416), and the high-performance computing resources of the Boston University Shared Computing Cluster (SCC). We thank the reviewers for insightful comments, which improved the overall quality of our manuscript.

AUTHOR DECLARATIONS

Conflict of Interest

The authors have no conflicts to disclose.

Author Contributions

Ayan Majumder: Conceptualization (equal); Data curation (equal); Formal analysis (equal); Writing – original draft (equal). **John E. Straub**: Conceptualization (equal); Project administration (lead); Supervision (lead); Writing – original draft (equal).

DATA AVAILABILITY

Initial structures of the membrane bilayer used in this study and the scripts used to generate the 3D potentials of mean force using well-tempered metadynamics are freely available at: https://github.com/ayan-majumder95/tm_metad.

REFERENCES

- ¹A. Majumder, N. Vuksanovic, L. C. Ray, H. M. Bernstein, K. N. Allen, B. Imperiali, and J. E. Straub, "Synergistic computational and experimental studies of a phosphoglycosyl transferase membrane/ligand ensemble," bioRxiv: 2023.05.07.539694 (2023).
- ²J.-L. Popot and D. M. Engelman, "Helical membrane protein folding, stability, and evolution," Annu. Rev. Biochem. 69, 881–922 (2000).
- ³G. B. Irvine, O. M. El-Agnaf, G. M. Shankar, and D. M. Walsh, "Protein aggregation in the brain: The molecular basis for Alzheimer's and Parkinson's diseases," Mol. Med. 14, 451–464 (2008).
- ⁴P. H. Nguyen, A. Ramamoorthy, B. R. Sahoo, J. Zheng, P. Faller, J. E. Straub, L. Dominguez, J.-E. Shea, N. V. Dokholyan, A. De Simone, B. Ma, R. Nussinov, S. Najafi, S. T. Ngo, A. Loquet, M. Chiricotto, P. Ganguly, J. McCarty, M. S. Li, C. Hall, Y. Wang, Y. Miller, S. Melchionna, B. Habenstein, S. Timr, J. Chen, B. Hnath, B. Strodel, R. Kayed, S. Lesné, G. Wei, F. Sterpone, A. J. Doig, and P. Derreumaux, "Amyloid oligomers: A joint experimental/computational perspective on Alzheimer's disease, Parkinson's disease, type II diabetes, and amyotrophic lateral sclerosis," Chem. Rev. 121, 2545–2647 (2021).
- ⁵C. Chipot, "Frontiers in free-energy calculations of biological systems," Wiley Interdiscip. Rev.: Comput. Mol. Sci. 4, 71–89 (2014).
- ⁶J. C. Gumbart, B. Roux, and C. Chipot, "Standard binding free energies from computer simulations: What is the best strategy?," J. Chem. Theory Comput. 9, 794–802 (2013).
- ⁷J. C. Gumbart, B. Roux, and C. Chipot, "Efficient determination of protein–protein standard binding free energies from first principles," J. Chem. Theory Comput. 9, 3789–3798 (2013).
- A. Filippov, G. Orädd, and G. Lindblom, "The effect of cholesterol on the lateral diffusion of phospholipids in oriented bilayers," Biophys. J. 84, 3079–3086 (2003).
 M. Lelimousin, V. Limongelli, and M. S. Sansom, "Conformational changes in the epidermal growth factor receptor: Role of the transmembrane domain investigated by coarse-grained metadynamics free energy calculations," J. Am. Chem. Soc. 138, 10611–10622 (2016).
- ¹⁰ J. Domański, G. Hedger, R. B. Best, P. J. Stansfeld, and M. S. Sansom, "Convergence and sampling in determining free energy landscapes for membrane protein association," J. Phys. Chem. B 121, 3364–3375 (2017).
- ¹¹A. Majumder and J. E. Straub, "Addressing the excessive aggregation of membrane proteins in the MARTINI model," J. Chem. Theory Comput. **17**, 2513–2521 (2021).
- ¹²A. Majumder, S. Kwon, and J. E. Straub, "On computing equilibrium binding constants for protein–protein association in membranes," J. Chem. Theory Comput. **18**, 3961–3971 (2022).
- ¹³V. Leone, F. Marinelli, P. Carloni, and M. Parrinello, "Targeting biomolecular flexibility with metadynamics," Curr. Opin. Struct. Biol. 20, 148–154 (2010).
- ¹⁴B. Roux, "The calculation of the potential of mean force using computer simulations," Comput. Phys. Commun. 91, 275–282 (1995).
- ¹⁵J. Comer, J. C. Gumbart, J. Hénin, T. Lelièvre, A. Pohorille, and C. Chipot, "The adaptive biasing force method: Everything you always wanted to know but were afraid to ask," J. Phys. Chem. B 119, 1129–1151 (2015).
- ¹⁶ J. Domański, M. S. Sansom, P. J. Stansfeld, and R. B. Best, "Balancing force field protein-lipid interactions to capture transmembrane helix-helix association," J. Chem. Theory Comput. 14, 1706–1715 (2018).
- ¹⁷D. Sengupta and S. J. Marrink, "Lipid-mediated interactions tune the association of glycophorin A helix and its disruptive mutants in membranes," Phys. Chem. Chem. Phys. 12, 12987–12996 (2010).
- ¹⁸ A. Barducci, G. Bussi, and M. Parrinello, "Well-tempered metadynamics: A smoothly converging and tunable free-energy method," Phys. Rev. Lett. 100, 020603 (2008).

- ¹⁹ K. R. MacKenzie, J. H. Prestegard, and D. M. Engelman, "A transmembrane helix dimer: Structure and implications," Science 276, 131–133 (1997).
- ²⁰ E. V. Bocharov, M. L. Mayzel, P. E. Volynsky, M. V. Goncharuk, Y. S. Ermolyuk, A. A. Schulga, E. O. Artemenko, R. G. Efremov, and A. S. Arseniev, "Spatial structure and pH-dependent conformational diversity of dimeric transmembrane domain of the receptor tyrosine kinase EphA1," J. Biol. Chem. 283, 29385–29395 (2008).
- ²¹ P. C. Souza, R. Alessandri, J. Barnoud, S. Thallmair, I. Faustino, F. Grünewald, I. Patmanidis, H. Abdizadeh, B. M. Bruininks, T. A. Wassenaar, P. C. Kroon, J. Melcr, V. Nieto, V. Corradi, H. M. Khan, J. Domański, M. Javanainen, H. Martinez-Seara, N. Reuter, R. B. Best, I. Vattulainen, L. Monticelli, X. Periole, D. P. Tieleman, A. H. de Vries, and S. J. Marrink, "Martini 3: A general purpose force field for coarse-grained molecular dynamics," Nat. Methods 18, 382–388 (2021).
- ²²G. A. Tribello, M. Bonomi, D. Branduardi, C. Camilloni, and G. Bussi, "PLUMED 2: New feathers for an old bird," Comput. Phys. Commun. 185, 604–613 (2014).
- ²³ M. J. Abraham, T. Murtola, R. Schulz, S. Páll, J. C. Smith, B. Hess, and E. Lindahl, "GROMACS: High performance molecular simulations through multi-level parallelism from laptops to supercomputers," Software X 1–2, 19–25 (2015).
- ²⁴M. Chavent, A. P. Chetwynd, P. J. Stansfeld, and M. S. Sansom, "Dimerization of the EphA1 receptor tyrosine kinase transmembrane domain: Insights into the mechanism of receptor activation," Biochemistry **53**, 6641–6652 (2014).
- ²⁵N. Castillo, L. Monticelli, J. Barnoud, and D. P. Tieleman, "Free energy of WALP23 dimer association in DMPC, DPPC, and DOPC bilayers," Chem. Phys. Lipids 169, 95–105 (2013).
- ²⁶J. Domański, M. S. Sansom, P. J. Stansfeld, and R. B. Best, "Atomistic mechanism of transmembrane helix association," PLoS Comput. Biol. **16**, e1007919 (2020).
- ²⁷K. G. Fleming, "Standardizing the free energy change of transmembrane helix-helix interactions," J. Mol. Biol. **323**, 563–571 (2002).
- 28 K. G. Fleming, A. L. Ackerman, and D. M. Engelman, "The effect of point mutations on the free energy of transmembrane α-helix dimerization," J. Mol. Biol. 272, 266–275 (1997).
- ²⁹ A. Nash, R. Notman, and A. M. Dixon, "De novo design of transmembrane helix-helix interactions and measurement of stability in a biological membrane," Biochim. Biophys. Acta, Biomembr. **1848**, 1248–1257 (2015).
- ⁵⁰H. Hong, T. M. Blois, Z. Cao, and J. U. Bowie, "Method to measure strong protein-protein interactions in lipid bilayers using a steric trap," Proc. Natl. Acad. Sci. U. S. A. 107, 19802–19807 (2010).

- ³¹S. Sarabipour and K. Hristova, "Glycophorin a transmembrane domain dimerization in plasma membrane vesicles derived from CHO, HEK 293T, and A431 cells," Biochim. Biophys. Acta, Biomembr. **1828**, 1829–1833 (2013).
- ³²L. Chen, L. Novicky, M. Merzlyakov, T. Hristov, and K. Hristova, "Measuring the energetics of membrane protein dimerization in mammalian membranes," J. Am. Chem. Soc. 132, 3628–3635 (2010).
- ³³L. Janosi, A. Prakash, and M. Doxastakis, "Lipid-modulated sequence-specific association of glycophorin A in membranes," Biophys. J. 99, 284–292 (2010).
- 34 J. Henin, A. Pohorille, and C. Chipot, "Insights into the recognition and association of transmembrane α -helices. The free energy of α -helix dimerization in glycophorin A," J. Am. Chem. Soc. 127, 8478–8484 (2005).
- 35 M. Javanainen, H. Martinez-Seara, and I. Vattulainen, "Excessive aggregation of membrane proteins in the Martini model," PLoS One 12, e0187936 (2017).
- ³⁶E. O. Artemenko, N. S. Egorova, A. S. Arseniev, and A. V. Feofanov, "Transmembrane domain of EphA1 receptor forms dimers in membrane-like environment," Biochim. Biophys. Acta, Biomembr. 1778, 2361–2367 (2008).
- ³⁷L. V. Schäfer, D. H. de Jong, A. Holt, A. J. Rzepiela, A. H. de Vries, B. Poolman, J. A. Killian, and S. J. Marrink, "Lipid packing drives the segregation of transmembrane helices into disordered lipid domains in model membranes," Proc. Natl. Acad. Sci. U. S. A. 108, 1343–1348 (2011).
- ³⁸Y. Yano and K. Matsuzaki, "Measurement of thermodynamic parameters for hydrophobic mismatch 1: Self-association of a transmembrane helix," Biochemistry **45**, 3370–3378 (2006).
- ³⁹H. Luo and K. Sharp, "On the calculation of absolute macromolecular binding free energies," Proc. Natl. Acad. Sci. U. S. A. **99**, 10399–10404 (2002).
- ⁴⁰E. Duboué-Dijon and J. Hénin, "Building intuition for binding free energy calculations: Bound state definition, restraints, and symmetry," J. Chem. Phys. **154**, 204101 (2021).
- 41 J. Henin, A. Pohorille, and C. Chipot, "Insights into the recognition and association of transmembrane α-helices. The free energy of α-helix dimerization in glycophorin A," J. Am. Chem. Soc. **132**, 9510 (2010).
- ⁴²J. S. Hub, B. L. De Groot, and D. van der Spoel, "g_wham—A free weighted histogram analysis implementation including robust error and autocorrelation estimates," J. Chem. Theory Comput. **6**, 3713–3720 (2010).
- ⁴³R. Trenker, M. E. Call, and M. J. Call, "Crystal structure of the glycophorin a transmembrane dimer in lipidic cubic phase," J. Am. Chem. Soc. 137, 15676–15679 (2015).
- ⁴⁴A. R. Sahoo, P. C. Souza, Z. Meng, and M. Buck, "Transmembrane dimers of type 1 receptors sample alternate configurations: MD simulations using coarse grain Martini 3 versus AlphaFold2 Multimer," Structure 31, 735–745.e2 (2023).